

Performance Modeling of MIMO OFDM Systems via Channel Analysis

Jie Gao, O. Can Ozdural, Sasan H. Ardalan, and Huaping Liu, *Member, IEEE*

Abstract—Multiple-input multiple-output (MIMO) antennas can be combined with orthogonal frequency division multiplexing (OFDM) to achieve diversity gain and/or to increase system spectral efficiency through spatial multiplexing. In this letter, we derive the probability density function (pdf) expressions of the condition number (i.e., the maximum-to-minimum-singular-value ratio, MMSVR) of the channel state information (CSI) matrix. We show that this ratio is directly related to the noise enhancement in open-loop MIMO systems and provides a significant insight on the overall system capacity. The pdf of this ratio could be used to predict the relative performances of various MIMO configurations without complex system-level simulations. The pdf can also be used to compute the probability of whether certain channels will fail in the high-throughput mode. Extensive simulations are performed to validate the accuracy of the closed-form pdf of the MMSVR derived in this letter.

Index Terms—Multiple-input multiple-output systems, orthogonal frequency division multiplexing, channel analysis, condition number, minimum mean-square error detection.

I. INTRODUCTION

IMPLEMENTATION of high-data-rate wireless local area network (WLAN) has been a major focus of research in recent years. Multiple-input multiple-output (MIMO) schemes [1]–[3] and orthogonal frequency division multiplexing (OFDM) [4] can be combined to operate at the high-throughput (HT) mode, or the diversity mode, or the combination of both in fading environments [5]. Such systems could achieve high spectral efficiency and/or a large coverage area that are critical for future-generation wireless local area networks.

Existing research has relied mainly on obtaining the error-rate performance curves to determine the throughput and diversity gains [6], [7] of various MIMO configurations, assuming Rayleigh fading and independent and identically distributed MIMO-OFDM sub-channels. Alternatively, the relative capacity and throughput of different system configurations can be obtained by using the channel characteristics. If analytical characterizations of the channel are available, this approach will be more efficient than the former, as it does not require complex system-level simulations.

Manuscript received November 19, 2004; revised March 23, 2005; accepted June 4, 2005. The associate editor coordinating the review of this letter and approving it for publication was A. Svensson.

J. Gao and O. Can Ozdural were with Intel Corporation while this work was performed. They are now with the School of Electrical Engineering and Computer Science, Oregon State University, Corvallis, OR 97331 USA (e-mail: gaoji@engr.orst.edu, ozdural@eecs.oregonstate.edu).

S. H. Ardalan is with the Wireless Networking Group, Intel Corporation, Hillsboro, OR 97124 USA (e-mail: sasan.h.ardalan@intel.com).

H. Liu is with the School of Electrical Engineering and Computer Science, Oregon State University, Corvallis, OR 97331 USA (e-mail: hliu@eecs.orst.edu).

Digital Object Identifier 10.1109/TWC.2006.04788.

Common open-loop linear detection schemes include the zero-forcing (ZF) and minimum mean-square error (MMSE) schemes [16], [17]. A large condition number (i.e., the maximum-to-minimum-singular-value ratio, MMSVR) of the channel state information (CSI) matrix implies a high noise enhancement and may cause the open-loop schemes to fail in exploiting the available capacity [8]. Thus, MMSVR could be a convenient and effective metric to characterize the performance of different MIMO configurations.

The importance and effectiveness of the eigenvalue distribution on MIMO system capacity and the overall system performance have been well recognized [9]–[12]. The eigenvalue analysis for MIMO-OFDM systems can be used to reduce the overall system complexity [13], [14]. In this letter, we derive the analytical probability density function (pdf) of the MMSVR value, which can be used to predict the relative performance of different MIMO configurations. The pdf can also be used to estimate the lower bound on the noise enhancement [15] and the capacity of MIMO channels. We establish the relationship between MMSVR and the achievable data throughput. Simulation results verify the accuracy of the closed-form pdf expressions of MMSVR derived in this letter.

This letter is organized as follows. In Section II, the MIMO-OFDM system model and the open-loop ZF and MMSE detection schemes [16], [17] will be described. Section III introduces the channel model and then derives the pdf of the MMSVR of the channel matrix, while Section IV provides simulation setup and discusses channel analysis simulation results for various MIMO configurations. Concluding remarks are made in Section V.

II. SYSTEM MODEL AND DETECTION SCHEMES

A. System Model

Consider a MIMO-OFDM system where the transmitter has N antennas, the receiver has M antennas, and all the transmitted symbols share K subcarriers. The frequency domain transmitted sequence from the n -th ($n = 1, \dots, N$) transmit antenna is represented by $X_{n,k}$, where $k = 1, \dots, K$ represents the k -th OFDM subcarrier. The sequence received by the m -th ($m = 1, \dots, M$) receive antenna is expressed as

$$Y_{m,k} = \sum_{n=1}^N H_{m,n,k} X_{n,k} + \zeta_{m,k} \quad (1)$$

where $H_{m,n,k}$ is the frequency response of the channel between the n -th transmit antenna and the m -th receive antenna for the k -th subcarrier, $\zeta_{m,k}$ is the frequency response of zero-mean additive white Gaussian noise (AWGN) with a one-sided power spectral density of \mathcal{N}_0 . Let us define the signal

transmitted on the k -th subcarrier from all the N transmit antennas as $\mathbf{X}_k = [X_{1,k}, X_{2,k}, \dots, X_{N,k}]^T$, where $(\cdot)^T$ denotes transpose. The received signal as a function of the respective CSI matrix \mathbf{H}_k can be expressed as

$$\begin{aligned} \mathbf{Y}_k &= [Y_{1,k}, Y_{2,k}, \dots, Y_{M,k}]^T \\ &= \begin{bmatrix} H_{1,1,k} & H_{1,2,k} & \dots & H_{1,N,k} \\ & & & \vdots \\ H_{M,1,k} & H_{M,2,k} & \dots & H_{M,N,k} \end{bmatrix} \mathbf{X}_k + \begin{bmatrix} \zeta_{1,k} \\ \zeta_{2,k} \\ \vdots \\ \zeta_{M,k} \end{bmatrix} \\ &= \mathbf{H}_k \mathbf{X}_k + \boldsymbol{\zeta}_k. \end{aligned} \quad (2)$$

We obtain the general system description by vertically stacking the received signal given in (2) for all K subcarriers as

$$\begin{aligned} \mathbf{Y} &= [\mathbf{Y}_1^T, \mathbf{Y}_2^T, \dots, \mathbf{Y}_K^T]^T \\ &= \mathbf{H} \mathbf{X} + \boldsymbol{\zeta} \end{aligned} \quad (3)$$

where $\mathbf{X} = [\mathbf{X}_1^T, \mathbf{X}_2^T, \dots, \mathbf{X}_K^T]^T$, $\boldsymbol{\zeta} = [\boldsymbol{\zeta}_1^T, \boldsymbol{\zeta}_2^T, \dots, \boldsymbol{\zeta}_K^T]^T$, and $\mathbf{H} = \text{diag}[\mathbf{H}_1, \mathbf{H}_2, \dots, \mathbf{H}_K]$ is a block diagonal matrix.

B. Detection

Open-loop detection schemes require $M \geq N$ if the system operates at the spatial multiplexing mode. ZF is the simplest open-loop method in which the estimates of the transmitted signals are obtained by multiplying the received signal \mathbf{Y} with the pseudo-inverse of the CSI matrix as

$$\hat{\mathbf{X}} = \mathbf{W}_{ZF} \mathbf{Y} = \mathbf{H}^+ \mathbf{Y} = \mathbf{X} + \boldsymbol{\xi} \quad (4)$$

where $(\cdot)^+$ represents the pseudo-inverse, $\mathbf{W}_{ZF} = \mathbf{H}^+$ is the weight matrix for the ZF scheme, and $\boldsymbol{\xi} = \mathbf{H}^+ \boldsymbol{\zeta}$. Note that the detection can be carried out on a subcarrier-by-subcarrier basis if there is no inter-carrier interference. This method requires channel estimates at the receiver, and since AWGN is not considered in the estimation process, it might result in a high noise enhancement. An MMSE receiver can be adopted to improve the performance of the ZF scheme. In the MMSE scheme, the weight matrix is $\mathbf{W}_{MMSE} = (\mathbf{H}^\dagger \mathbf{H} + \mathcal{N}_0 \mathbf{I}_{NK})^{-1} \mathbf{H}^\dagger$, where $(\cdot)^\dagger$ denotes Hermitian transpose and \mathbf{I}_{NK} is the $NK \times NK$ identity matrix. In the extreme case when signal-to-noise ratio equals infinity, the ZF scheme is the same as the MMSE scheme. At high signal-to-noise ratios (SNR), the instantaneous noise power of the n -th data stream transmitted on the k -th subcarrier is written as [18]

$$E\{\boldsymbol{\xi} \boldsymbol{\xi}^\dagger\}_{n \times k, n \times k} = \mathcal{N}_0 [\mathbf{W} \mathbf{W}^\dagger]_{n \times k, n \times k} \quad (5)$$

where $[\cdot]_{n \times k, n \times k}$ denotes the $(n \times k, n \times k)$ -th component of a matrix, $E\{\cdot\}$ denotes expectation, and \mathbf{W} could be either \mathbf{W}_{ZF} or \mathbf{W}_{MMSE} . For a particular CSI matrix \mathbf{H} , the instantaneous noise enhancement factor for the n -th data stream in the k -th subcarrier is $[\mathbf{W} \mathbf{W}^\dagger]_{n \times k, n \times k}$. When the MMSVR of \mathbf{H} is large, the noise enhancement will be high.

III. ANALYSIS OF MIMO CHANNEL

A. Channel Model

Spatial sub-channels (i.e., the channel from transmit antenna n to receive antenna m) are assumed to be independent. This

assumption is valid if the antenna spacing is greater than half of the wavelength of the carrier. We adopt the IEEE 802.11 model with an exponential power-delay profile [20]. The channel is modeled as a finite impulse response (FIR) filter where all the $L + 1$ paths are independent complex Gaussian random variables with zero mean and average power ω_l^2 ($l = 0, 1, \dots, L$). The channel impulse response can be written as $h_l = a + jb$, where a and b are defined to be random variables obeying normal distribution with zero mean and variance of $\omega_l^2/2$. In this model, the power of multipath components decreases exponentially. To normalize the channel energy, the first multipath component is chosen as $\omega_0^2 = (1 - \beta)/(1 - \beta^{L+1})$, where $\beta = e^{-T_s/\tau_{rms}}$, $L = 10\tau_{rms}/T_s$, T_s represents the sampling period, and τ_{rms} is the root mean-square (RMS) delay spread of the channel. The energy of the l -th multipath component is then defined as $\omega_l^2 = \omega_0^2 \beta^l$.

B. Analysis of channel characteristics

For the ZF and MMSE detection schemes to work efficiently, some constraints must be met. First of all, the number of receive antennas M should not be, as mentioned earlier, less than the number of transmit antennas N . In the downlink of a practical WLAN system, however, it is preferred to have more antennas at the transmitter considering power consumption of the receiver. Moreover, the CSI matrix for each subcarrier, \mathbf{H}_k , should not be an ill-conditioned¹ matrix since such a matrix will cause a high noise enhancement in detection. For open-loop operations, the system could run in the HT mode (the number of spatial streams equals the number of transmit antennas) when the received SNR is moderately high. If the channel is ill-conditioned, detection using the ZF or MMSE scheme will experience a low instantaneous SNR, resulting in poor performance. In this case, it might be better to switch the system to operate at the diversity mode (the number of spatial streams is less than the number of transmit antennas).

Let the noise enhancement matrix for the k -th subcarrier be $\boldsymbol{\Omega}_k$, $k = 1, \dots, K$. For a rank-two² ZF scheme in the HT mode, using the singular value decomposition (SVD) of the CSI matrix, we obtain $\boldsymbol{\Omega}_{ZF,k}$ as

$$\begin{aligned} \boldsymbol{\Omega}_{ZF,k} &= \mathbf{W}_{ZF,k} \mathbf{W}_{ZF,k}^\dagger = \mathbf{H}_k^+ (\mathbf{H}_k^+)^{\dagger} = (\mathbf{H}_k^\dagger \mathbf{H}_k)^+ \\ &= (\mathbf{V}_k \boldsymbol{\Sigma}_k^\dagger \mathbf{U}_k^\dagger \mathbf{U}_k \boldsymbol{\Sigma}_k \mathbf{V}_k^\dagger)^+ \\ &= \mathbf{V}_k (\boldsymbol{\Sigma}_k^\dagger \boldsymbol{\Sigma}_k)^+ \mathbf{V}_k^\dagger \\ &= \mathbf{V}_k \begin{bmatrix} 1/|\sigma_{k,1}|^2 & 0 \\ 0 & 1/|\sigma_{k,2}|^2 \end{bmatrix} \mathbf{V}_k^\dagger \\ &= |\sigma_{k,1}|^{-2} \mathbf{V}_k \begin{bmatrix} 1 & 0 \\ 0 & |\sigma_{k,1}|^2/|\sigma_{k,2}|^2 \end{bmatrix} \mathbf{V}_k^\dagger \end{aligned} \quad (6)$$

where $\sigma_{k,1}$ and $\sigma_{k,2}$ ($\sigma_{k,1} \geq \sigma_{k,2} > 0$) represent the singular values of matrix \mathbf{H}_k . $1/|\sigma_{k,1}|^2$ and $1/|\sigma_{k,2}|^2$ also represent the noise enhancement factors for the two sub-channels. Let $\gamma_k = \sigma_{k,1}/\sigma_{k,2}$. A large γ_k value could arise either because $\sigma_{k,2}$ is small or because $\sigma_{k,1}$ is large. From simulation

¹In this letter, a non-square matrix is defined to be ill-conditioned if the minimum singular value of the channel matrix is significantly small compared to the maximum singular value.

²The main focus of this letter is on rank-two and rank-three CSI matrices since the emerging IEEE 802.11n MIMO WLAN standard is expected to have 2 to 4 transmit and 2 to 4 receive antennas.

results, it is found that the latter is unlikely³, thus γ_k is a good indicator of noise enhancement, and if $\gamma_k \gg 1$, we can conclude that the channel is ill-conditioned for the k -th subcarrier. For an open-loop system with a rank higher than two, the definition of γ_k can be generalized as $\sigma_{k,1}/\sigma_{k,u}$, where $u = \min(N, M)$, and $\sigma_{k,1}$, $\sigma_{k,u}$ are the maximum and minimum singular values, respectively.

MMSVR is also a good measure of the system capacity lower bound. Using the alternative capacity representation of [9], the capacity of the k -th carrier can be written as

$$C_k = \sum_{i=1}^u \log_2 \left(1 + \frac{P_k}{N} |\sigma_{k,i}|^2 \right) \quad (7)$$

where P_k is the total power of the k -th subcarrier. Considering $\sigma_{k,1} \geq \sigma_{k,2} \geq \dots \geq \sigma_{k,u} > 0$, a lower bound of the capacity can be written as

$$C_k \geq \log_2 \left(1 + \frac{P_k}{N} |\sigma_{k,1}|^2 \right) + (u-1) \log_2 \left(1 + \frac{P_k}{N} \frac{|\sigma_{k,1}|^2}{|\gamma_k|^2} \right). \quad (8)$$

As mentioned earlier, a large γ_k value is mostly due to a small $\sigma_{k,u}$ value. This fact combined with Eq. (8) clearly indicates that a high value of MMSVR results in a considerably lowered system capacity.

The Fourier transform of the channel impulse response of each OFDM carrier described in Section III-A has a normal distribution. The singular values of the CSI matrix for the k -th OFDM carrier, \mathbf{H}_k , are the positive square-roots of the eigenvalues of the positive-definite Wishart matrix given as $\mathbf{Q}_k = \mathbf{H}_k^\dagger \mathbf{H}_k$, where $(\cdot)^\dagger$ represents Hermitian transpose. To obtain the pdf of γ_k , the joint pdf of the eigenvalues of \mathbf{Q}_k is needed. Let $\lambda_1 \geq \lambda_2 \geq \dots \geq \lambda_u$ be the eigenvalues of the positive-definite matrix \mathbf{Q}_k . The joint density function of $\lambda_1, \lambda_2, \dots, \lambda_u$ are obtained to be

$$f_\lambda(\lambda_1, \dots, \lambda_u) = K_{u,v}^{-1} e^{-\sum_i \lambda_i} \prod_i \lambda_i^{v-u} \prod_{i < j} (\lambda_i - \lambda_j)^2 \quad (9)$$

where $u = \min(N, M)$, $v = \max(N, M)$, and $K_{u,v}$ is a normalization factor [9]. From Eq. (9), we can calculate the joint density function of λ_1 and λ_u , $f_\lambda(\lambda_1, \lambda_u)$, from which the joint cumulative distribution function is obtained as

$$F_\lambda(\lambda_1, \lambda_u) = \int_0^{\lambda_1} \int_0^{\lambda_u} f_\lambda(\alpha, \beta) d\alpha d\beta. \quad (10)$$

Since the singular values of \mathbf{H}_k , σ_i , $i = 1, \dots, u$, are the square-root of the eigenvalues λ_i , $i = 1, \dots, u$, of the positive-definite matrix \mathbf{Q}_k , the joint cumulative distribution of σ_1 and σ_u is

$$\begin{aligned} F_\sigma(\sigma_1, \sigma_u) &= P(\sqrt{\lambda_1} \leq \sigma_1, \sqrt{\lambda_u} \leq \sigma_u) \\ &= P(0 \leq \lambda_1 \leq \sigma_1^2, 0 \leq \lambda_u \leq \sigma_u^2) \\ &= F_\lambda(\sigma_1^2, \sigma_u^2) - F_\lambda(0, \sigma_u^2) - \\ &\quad F_\lambda(\sigma_1^2, 0) + F_\lambda(0, 0). \end{aligned} \quad (11)$$

³The probability of having $\sigma_{k,1}$ larger than five equals 8.71×10^{-9} for a 2×2 system, 1.05×10^{-7} for a 2×3 system, 1.17×10^{-6} for a 3×3 system, 8.59×10^{-6} for a 3×4 system, 5.81×10^{-5} for a 4×4 system and 2.92×10^{-4} for a 4×5 system.

Using Eq. (11), the probability density function of γ , omitting the subscript for simplicity of notation in the sequel, can be derived as

$$f_\sigma(\sigma_1, \sigma_u) = \frac{d^2 F_\sigma(\sigma_1, \sigma_u)}{d\sigma_1 d\sigma_u} \quad (12)$$

$$\begin{aligned} f_\gamma(\gamma) &= f_\sigma \left(\frac{\sigma_1}{\sigma_u} \right) \\ &= \int_0^\infty |\sigma_u| f_\sigma(\sigma_u \gamma, \sigma_u) d\sigma_u. \end{aligned} \quad (13)$$

For 2×2 and 2×3 configurations, the distribution of the singular value ratios obtained using Eqs. (9)-(13) are

$$f_\gamma(\gamma)_{2 \times 2} = \frac{12\gamma(-1+\gamma^2)^2}{(1+\gamma^2)^4} \quad (14)$$

$$f_\gamma(\gamma)_{2 \times 3} = \frac{120\gamma^3(-1+\gamma^2)^2}{(1+\gamma^2)^6}. \quad (15)$$

Similarly for 3×3 and 3×4 systems, the distributions of γ obtained by using Eqs. (9)-(13) are

$$f_\gamma(\gamma)_{3 \times 3} = \frac{216(-1+\gamma^2)^7(1+\gamma^2)(11+20\gamma^2+11\gamma^4)}{(2+5\gamma^2+2\gamma^4)^6} \quad (16)$$

$$f_\gamma(\gamma)_{3 \times 4} = \frac{840\gamma^3(-1+\gamma^2)^7(1+\gamma^2)(A_{3 \times 4}(\gamma) + B_{3 \times 4}(\gamma))}{(2+5\gamma^2+2\gamma^4)^9} \quad (17)$$

where

$$A_{3 \times 4}(\gamma) = 4107\gamma^2 + 11562\gamma^4 + 15868\gamma^6 \quad (18a)$$

$$B_{3 \times 4}(\gamma) = 454 + 11562\gamma^8 + 4107\gamma^{10} + 454\gamma^{12}. \quad (18b)$$

The methodology of calculating the closed-form theoretical expressions for the pdf of γ can be easily extended to MIMO-OFDM systems with a rank higher than three.

IV. SIMULATION RESULTS AND DISCUSSION

In simulations, an RMS delay spread of $\tau_{rms} = 50$ ns and the maximum delay of $10\tau_{rms}$ are considered. Statistics are collected based on 10,000 channel realizations. Each channel tap is modeled as an independent complex Gaussian random variable. The CSI matrix is decomposed on a per OFDM carrier basis, and as defined in Section III-B, γ_k is the ratio of the maximum and the minimum singular values of \mathbf{H}_k for the k -th subcarrier. The parameters of OFDM symbols are chosen as in the IEEE 802.11a standard (i.e., 64 subcarriers in one OFDM symbol with a subcarrier frequency spacing of 312.5kHz).

The analytical and simulated pdf of γ_k , $k = 1, \dots, 64$, for a 2×2 system and a 2×3 system are shown in Fig. 1. For both cases, the simulation and analytical results match very well. Fig. 2 shows the simulation and theoretical results for the system with 3 transmit antennas.

The pdf of γ leads directly to results showing which $N \times M$ MIMO configuration is an appropriate choice for the high-throughput mode. For instance, it is well known that an $N \times (M+1)$ open-loop MIMO scheme outperforms an $N \times M$ system. The pdf of γ derived in this letter confirms this result. For example, the pdf of γ clearly demonstrates that a 2×2 spatial multiplexing system will experience a much higher

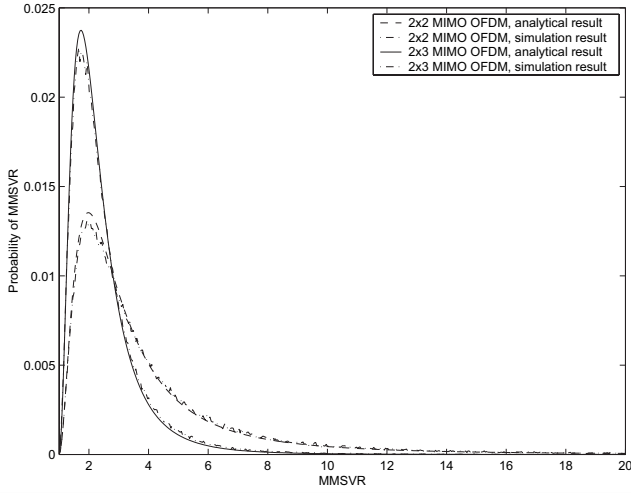


Fig. 1. Analytical and simulated probability density of MMSVR for 2×2 and 2×3 MIMO-OFDM configurations.

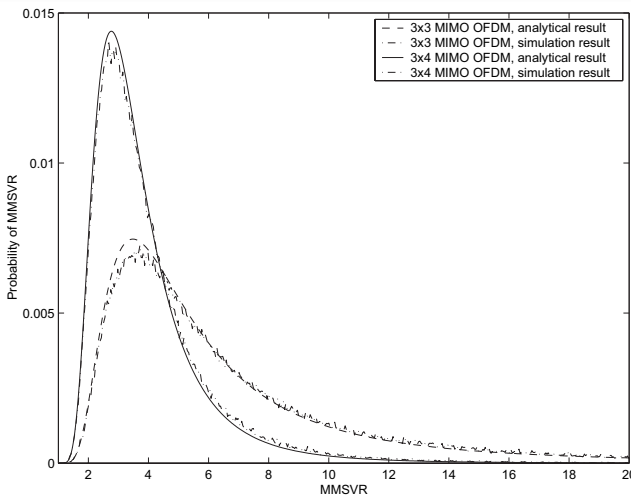


Fig. 2. Analytical and simulated probability density of MMSVR for 3×3 and 3×4 MIMO OFDM configurations.

probability of having an ill-conditioned channel compared to a 2×3 system. A 3×3 configuration is found to have a much higher probability of ill-conditioned channels compared to a 2×2 system, even though the former has a higher throughput.

The difference of noise enhancement between two MIMO configurations will result in different throughput. It is shown in [15] that the lower bound of the noise enhancement when ZF detection is adopted is given as the mean of the square of MMSVR. This bound can be calculated using the analytical expression of the pdf of MMSVR as

$$E\{\gamma_{N \times M}^2\} = \int_1^\infty \gamma^2 f_\gamma(\gamma_{N \times M}) d\gamma. \quad (19)$$

The mean value of $\gamma_{N \times M}^2$ is calculated to be 19.9636, 7.5452, 41.1853 and 17.9986 for 2×2 , 2×3 , 3×3 and 3×4 MIMO configurations, respectively. Using these results, the relative throughput gains can be estimated through channel analysis as $10 \log_{10}(E\{\gamma_{N \times N}^2\}) - 10 \log_{10}(E\{\gamma_{N \times (N+1)}^2\})$. Figs. 3 and 4 show the upper bound of the throughput curves of

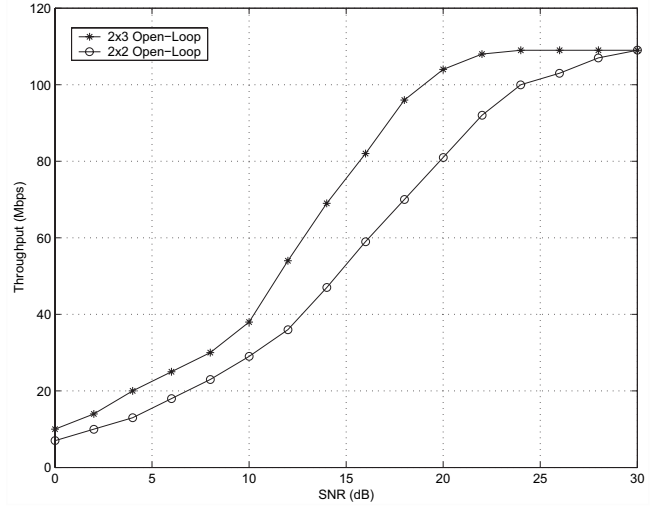


Fig. 3. Throughput comparison of MIMO-OFDM systems at 20MHz [19].

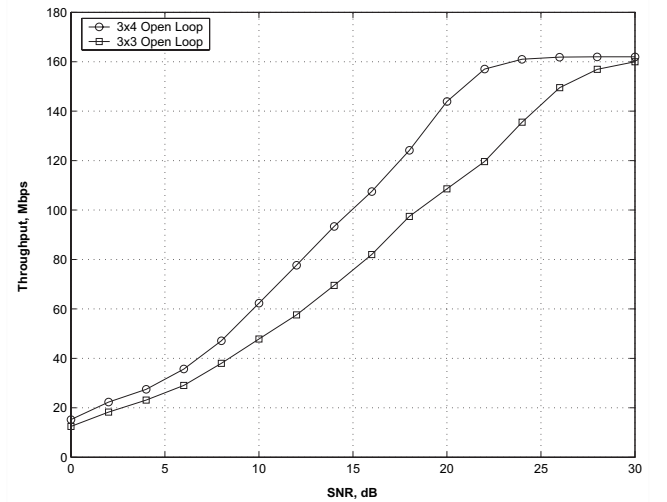


Fig. 4. Throughput comparison of MIMO-OFDM systems at 20MHz [19].

MIMO-OFDM schemes versus SNR⁴. It is observed that for a throughput of 80Mbps, the 2×3 system attains an approximate 4.2dB gain over the 2×2 system, and the 3×4 has a gain of 3.6dB over the 3×3 system. These results match well with the results obtained by using Eq. (19): 4.2257dB gain for 2×3 over 2×2 , and 3.5950dB gain for 3×4 over 3×3 . The improvement provided by an extra receive antenna is attributed to having fewer ill-conditioned channels.

V. CONCLUSION

We have derived the closed-form pdf expressions of the condition number (MMSVR) of the channel matrix for various MIMO configurations. These analytical results can be used to predict the relative performance of MIMO-OFDM systems

⁴Five thousand channel realizations are created. For each realization, the throughput of each modulation coding scheme (MCS) is calculated. After obtaining the packet error rate (PER) using the i -th MCS, the corresponding throughput is calculated as $Throughput(i) = D(i) * (1 - PER(i))$, where $D(i)$ is data rate provided by the i -th MCS. The maximum throughput value over all MCS sets is adopted as the ideal hull throughput for a specific realization [19].

without complicated system-level simulations. They can also be applied to determine the lower capacity bound of such systems. Through the channel analysis, it is clearly observed that an additional receive antenna could provide significant performance improvements. The analytical results and the gain/loss of different configurations predicted using the mean of the square of MMSVR matches well that obtained through system-level simulations. The results presented in this letter provide a simple and effective way for predicting the relative performances of different MIMO-OFDM configurations.

REFERENCES

- [1] A. Pualraj, D. Gore, R. Nabar, and H. Bölcskei, "An overview of MIMO communications - a key to gigabit wireless," in *Proc. IEEE 2004*, vol. 92, pp. 198–218.
- [2] A. Goldsmith, S. Jafar, N. Jindal, and S. Vishwanath, "Capacity limits of MIMO channels," *IEEE J. Select. Areas Commun.*, vol. 21, pp. 684–702, June 2003.
- [3] "Supplement to IEEE standard for information technology telecommunications and information exchange between systems - local and metropolitan area networks - specific requirements. Part 11: wireless LAN Medium Access Control (MAC) and Physical Layer (PHY) specifications: high-speed physical layer in the 5 GHz band," *IEEE Std 802.11a-1999*, Dec. 1999.
- [4] G. Stüber, J. Barry, S. McLaughlin, Y. Li, M. Ingram, and T. Pratt, "Broadband MIMO-OFDM wireless communications," in *Proc. IEEE 2004*, vol. 92, pp. 271–294.
- [5] A. van Zelst and T. Schenk, "Implementation of a MIMO OFDM-Based Wireless LAN System," *IEEE Trans. Signal Processing*, vol. 52, pp. 483–494, Feb. 2004.
- [6] L. Zheng and D. N. C. Tse, "Diversity and multiplexing: a fundamental tradeoff in multiple-antenna channels," *IEEE Trans. Inform. Theory*, vol. 49, pp. 1073–1096, May 2003.
- [7] R. Heath, Jr. and A. Paulraj, "Switching between multiplexing and diversity based on constellation distance," in *Proc. Allerton Conference on Communication, Control and Computing 2000*.
- [8] H. Artes, D. Seethaler and F. Hlawatsch, "Efficient detection algorithms for MIMO channels: a geometrical approach to approximate ML detection," *IEEE Trans. Signal Processing*, vol. 51, pp. 2808–2820, Nov. 2003.
- [9] I. E. Telatar, "Capacity of multi-antenna Gaussian channels," *European Trans. Telecomm. Related Technol.*, vol. 10, pp. 585–595, Nov.-Dec. 1999.
- [10] M. Chiani, M. Z. Win, and A. Zanella, "The distribution of eigenvalues of a Wishart matrix with correlation and application to MIMO capacity," in *Proc. IEEE Globecom'03*, pp. 1802–1805.
- [11] C. Martin and B. Ottersten, "Asymptotic eigenvalue distribution and capacity for MIMO channels under correlated fading," *IEEE Trans. Wireless Commun.*, vol. 3, pp. 1350–1359, July 2004.
- [12] R. K. Malik, "The pseudo-Wishart distribution and its application to MIMO systems," *IEEE Trans. Inform. Theory*, vol. 49, pp. 2761–2769, Oct. 2003.
- [13] D. Huang and K. B. Letaief, "Pre-DFT processing using eigen-analysis for coded OFDM with multiple receive antennas," *IEEE Trans. Commun.*, vol. 52, pp. 2019–2027, Nov. 2004.
- [14] D. Huang and K. B. Letaief, "Symbol based space diversity for coded OFDM systems," *IEEE Trans. Wireless Commun.*, vol. 3, pp. 117–127, Jan. 2004.
- [15] C. Mecklenbrauker and M. Rupp, "Generalized Alamouti codes for trading quality of service against data rate in MIMO UMTS," *Eurasip Journal of Applied Signal Processing: Special Issue on MIMO Comm. and Signal Processing*, pp. 662–675, May 2004.
- [16] B. Bjerke and J. Proakis, "Multiple-antenna diversity techniques for transmission over fading channels," in *Proc. IEEE Wireless Communications and Networking Conference 1999*, vol. 3, pp. 1038–1042.
- [17] D. Gesbert, M. Shafi, D. Shiu, P. Smith, and A. Naguib, "From theory to practice: an overview of MIMO spacetime coded wireless systems," *IEEE J. Select. Areas Commun.*, vol. 21, pp. 281–302, Apr. 2003.
- [18] H. Liu, "Error performance of MIMO systems in frequency selective Rayleigh fading channels," in *Proc. IEEE Globecom'03*.
- [19] A. Maltsev and A. Davydov, "MIMO-OFDM system performance," *TR 03-05 Intel Nizhny Novgorod Labs (INNl)*, Nov. 2003.
- [20] S. Halford, K. Halford, and M. Webster, "Evaluating the performance of HRb proposals in the presence of multipath," *doc: IEEE 802.11-00/282r2*, Sept. 2000.